Tamm surface states in a finite chain of defects in a photonic crystal

2007 J. Phys.: Condens. Matter 19 056004

(http://iopscience.iop.org/0953-8984/19/5/056004)

INSTITUTE OF PHYSICS PUBLISHING JOURNAL OF PHYSICS: CONDENSED MATTER

J. Phys.: Condens. Matter **19** (2007) 056004 (12pp) doi:10.1088/0953-8984/19/5/056004

Tamm surface states in a finite chain of defects in a photonic crystal

N Malkova and C Z Ning

NASA Ames Research Center, Moffett Field, CA 94035, USA
and
Center for Nanophotonics, Department of Electrical Engineering, Arizona State University, Tempe, AZ 85287, USA

E-mail: nmalkova@mail.arc.nasa.gov and cning@asu.edu

Received 23 September 2006, in final form 22 November 2006
Published 15 January 2007
Online at stacks.iop.org/JPhysCM/19/056004

Abstract

We present detailed theoretical and numerical studies of surface states of a coupled defect chain of finite length in a photonic crystal. By comparatively studying three such structures with zero, one, and two defects on the photonic crystal surface, respectively, we found that the transmission characteristics of the structure depend on the termination of the defect chain in the host crystal. The peak frequencies and the number of peaks are related to the boundary conditions of the coupled defects. Our numerical simulations in conjunction with analytical treatment using the coupled mode theory fully establish the analogy between the surface states in photonic crystals and the Tamm states in solids. We also point out how the results of the localized surface states in this one-dimensional model system can be generalized to two- or three-dimensional systems where surface states become surface waves.

(Some figures in this article are in colour only in the electronic version)

1. Introduction

The surface excitations (discrete states or continuous waves) supported by a periodical dielectric structure or photonic crystal (PC), which are referred to as surface Bloch states (SBSs), have attracted increasing attention due to their importance in many applications [1]. Existence of the SBSs was first demonstrated for one-dimensional PCs [2–4]. The SBSs were also identified theoretically and experimentally in two-dimensional PCs [5–8]. It was shown that the SBSs can either decay in the air and into the PC, or decay into the PC but extend in the air [5]. In a two-dimensional photonic crystal, the SBSs have only been observed either in PCs terminated by 'half-rods' (or hemicylindrical rods) [6], or by a surface mono-layer with smaller radius of the rods [9]. However, the underlying physics of the SBSs is still under debate [10]. It is also unclear how and to what extent the SBSs can be controlled. For example, we may ask why hemicylindrical termination of photonic crystal results in well defined surface states

inside the bandgap, while a cut throughout the end cylinders with smaller or larger than the half-cylinder would not lead to any surface state.

Since the SBSs are related to periodical structures, they could be considered analogous to the surface states in solids. The localized states at the surface of solids can be either Tamm-like [11] or Shockley-like [12] states. The Tamm states are caused by the strong perturbation at the surface, leading to an asymmetric potential with respect to the surface, while the Shockley states appear even without such an asymmetry, due to the so called anti-crossing of bands formed by different orbitals [13]. It was suggested to consider the SBSs on multilayer structures (one-dimensional PCs) as analogous to the surface Shockley states in solids [3]. However, this analogy cannot explain the fact that the surface states can appear inside the bandgap only when the separation between the layers is large enough. In contrast, the main condition for the Shockley electronic surface states is that the interatomic distance becomes small enough that the boundary curves of the allowed energy bands have crossed [12].

In a recent attempt [14] to understand the underlying physics of the SBSs, we followed the approach suggested first by Tamm in solids [11] and reduced the surface state problem to a one-dimensional one. We investigated the SBSs of defect chains in a PC. We showed that the surface states of the chain composed of identical defects are closely related to the Tamm surface states in solids rather than to the Shockley surface states. In this context, it is important to note that nowadays the researchers from a number of groups [15] try to connect so-called surface solitons, which appear on the surface or interface of periodical arrays of the nonlinear waveguides, and the Tamm surface states in solids, solely using the analogy in the termination of the periodical dielectric and atomic potentials. However, the nature of the surface states is determined by the surface potential, more specifically by its asymmetry with respect to the coupling constant (or width of the relevant allowed band) [13]. Hence a proof of the Tamm-like character of the surface states (and therefore their essential properties) should be based on analysis of the surface potential. Such an analysis will be a subject of the present paper.

In addition to serving as a one-dimensional model system for surface states to eventually understand those in two- and three-dimensional PCs, the understanding of light localization at the ending defects of a one-dimensional chain is also of great importance in its own right as an important type of waveguides, the coupled defect waveguides. Therefore, the goal of this paper is also to analyse in full detail the localized surface states of a defect chain to understand the transmission and reflection of such waveguides. Our model system is a two-dimensional PC doped with a chain of equidistant and identical defects (figure 1). In terms of the tight-binding model, such a structure can be described by the Bloch wavefunctions built on the localized eigenstates of the defects [16]. We choose defects that support a non-degenerate s-like mode inside the bandgap of the perfect crystal. The spectrum of the defect chain does not depend on the momentum parallel to the crystal surface (y-axis in figure 1). Because of this, the surface states of the chain, being localized on the ending defects, cannot propagate along the crystal surface. We focus on how the termination of the defect chain inside the host PC affects the eigenspectrum of the structure. In order to analyse this structure we use the finite difference time domain technique (FDTD) and empirical tight-binding model. Through the detailed analytical and numerical analyses we demonstrate the Tamm-like properties of the surface states in such structures. We will also discuss the possible extension of our approach to the case of the propagating surface states (waves) in a two-dimensional PC.

The paper is organized as follows. In section 2 we describe the model systems to be studied and present the tight-binding analysis of the surface states in PCs. In section 3, we present the FDTD simulations and explain the numerical results in terms of the tight-binding model. In section 4 we discuss the possible extensions of our approach. Section 5 concludes the paper with a summary of the main results.

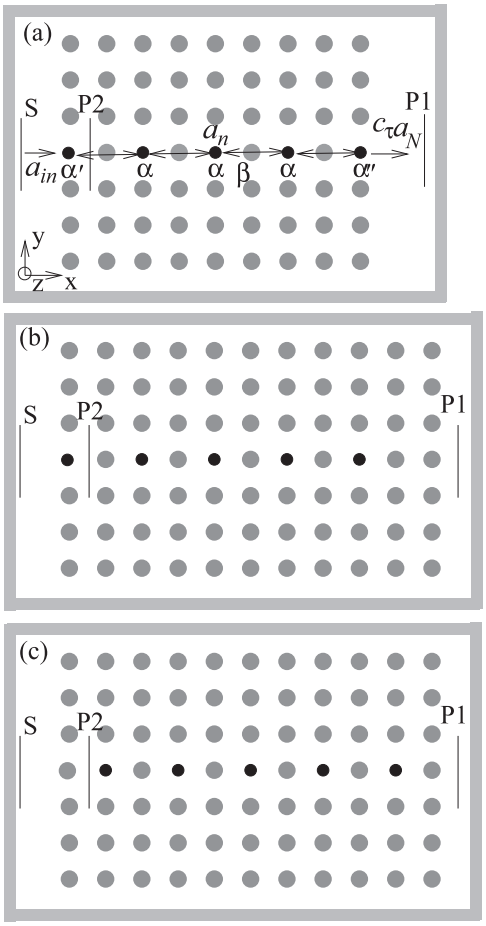

Figure 1. (a)–(c) Structures 1, 2, and 3, respectively. The source (S), two ports (P1, P2), perfect matched layers (the grey boxes), and frame of the reference system are shown.

2. Surface states of a defect chain

The structures to be discussed are shown in figure 1. The two-dimensional PC is a periodical array of infinitely long dielectric rods (grey dots) embedded in another dielectric medium. This otherwise perfect PC is doped with a chain of identical and equidistant defect rods (black dots). We can design this structure in such a way that the defect chain would generate the split defect states (or the allowed band of the chain) inside the bandgap of the host crystal. Then, as a first-order approximation, we neglect the coupling between the defect rods and the perfect PC. Therefore, we can consider this structure as a periodical array (chain in our case) embedded in another quasi-homogeneous medium (perfect PC). Depending on the termination of the defect chain, we distinguish structures 1, 2, and 3, as shown in figures 1(a), (b), and (c).

We first consider the infinite chain of the identical defects separated by distance d in the framework of the tight-binding model [17]. The wavefunction of the chain is represented as a linear combination of the eigenmodes, $\phi(r - nd)$, of the individual defects at the nth site, $\Psi(r, t) = \sum_n a_n(t)\phi(r - nd)$. In the nearest-neighbour approximation (see figure 1(a)), the dynamics of the field amplitude $a_n(t)$ at the nth defect can be characterized by the following

set of ordinary differential equations [17]:

$$\mathrm{i}\frac{\mathrm{d}}{\mathrm{d}t}a_n = \alpha a_n + \beta(a_{n-1} + a_{n+1}), \tag{1}$$

where $\alpha = \omega_0 - \mathrm{i}\gamma_0$ is the complex eigenvalue of the individual defect defined by the frequency, ω_0, and width, γ_0, of the resonant peak. If an individual defect is characterized by a single mode, the coupling between the nearest defect modes $\phi_n = \phi(r - nd)$ and ϕ_{n-1} is represented by the matrix element

$$\beta = \omega_0 \frac{\int \mathrm{d}\vec{r}\, \delta\epsilon\phi_n\phi_{n-1}}{\int \mathrm{d}\vec{r}\, \epsilon|\phi_n|^2}. \tag{2}$$

Here ϵ is the spatial distribution of the dielectric constant in the single-defect PC, and $\delta\epsilon$ is the dielectric constant change between the host crystal and defect rod. For an infinite chain of defects, the solution of the problem takes the form

$$a_n(t) = A_n \exp(-\mathrm{i}\omega t) = a_- \exp[\mathrm{i}kdn - \mathrm{i}\omega t] + a_+ \exp[-\mathrm{i}kdn - \mathrm{i}\omega t]. \tag{3}$$

Here k is the momentum defined by the dispersion relation

$$\omega = \alpha - 2\beta\cos(kd). \tag{4}$$

In the case of a finite chain with N defects, all defects in the chain are identical except the two defects on the ends, which are described by the following two equations:

$$\begin{aligned} \mathrm{i}\frac{\mathrm{d}}{\mathrm{d}t}a_1 &= \alpha' a_1 + \beta' a_2 + \tau a_{\mathrm{in}}, \\ \mathrm{i}\frac{\mathrm{d}}{\mathrm{d}t}a_N &= \alpha'' a_N + \beta'' a_{N-1}, \end{aligned} \tag{5}$$

where α', α'', and β', β'' are the eigenvalues and coupling constants of the end defects, respectively. In the equation for the first defect the extra term, τa_{in} represents the portion τ of the input excitation, a_{in}, which reaches the first defect from the source (see figure 1(a)). The transmitted field from the chain can be defined as a portion c_τ of the field amplitude at the last defect. Then, by assuming $\beta'' = \beta' = \beta$, we get the relative transmission of the N-defect chain as

$$T = \frac{c_\tau \tau\beta \sin kd}{(\alpha'' - \omega)(\alpha' - \omega)\sin[(N-1)kd] + \beta(\alpha'' + \alpha' - 2\omega)\sin(Nkd) + \beta^2 \sin[(N+1)kd]}. \tag{6}$$

Finally, using the ansatz of (3) and assuming $a_{\mathrm{in}} = 0$, we reduce the set of equations (1), (5) to the $N \times N$ eigenvalue problem which defines the spectrum ω and amplitude A_n of the defect chain:

$$\begin{pmatrix} \alpha' - \omega & \beta' & 0 & \cdots & 0 & 0 \\ \beta' & \alpha - \omega & \beta & \cdots & 0 & 0 \\ 0 & \beta & \alpha - \omega & \beta & \cdots & 0 \\ \vdots & \vdots & \vdots & \vdots & \vdots & \vdots \\ 0 & 0 & \cdots & \beta & \alpha - \omega & \beta'' \\ 0 & 0 & \cdots & 0 & \beta'' & \alpha'' - \omega \end{pmatrix} \begin{pmatrix} A_1 \\ A_2 \\ A_3 \\ \cdots \\ A_{N-1} \\ A_N \end{pmatrix} = 0. \tag{7}$$

We next would like to understand how the properties of the N-defect chain will change with increasing values of $|\alpha' - \alpha|$ and $|\alpha'' - \alpha|$. First of all, we note that in terms of mathematics the eigenvalue problem (7) is equivalent to the tight-binding problem for the electron states in a one-dimensional periodical potential with N atoms [13]. The termination of the periodical potential by the surface is introduced via the assumption that the Coulomb integral is different

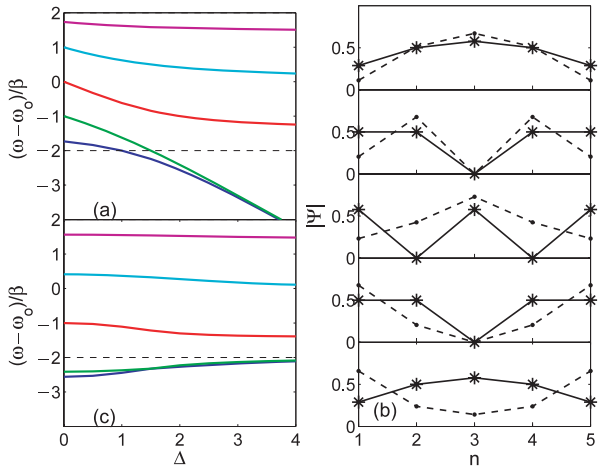

Figure 2. Energy spectrum of a five-defect chain. The energy levels versus parameter $\Delta = |\alpha - \alpha'|/\beta$ without (a) and with (c) the decay process. The dashed line shows the bottom of the allowed band. (b) The absolute value of the wavefunctions neglecting the decay for each eigenvalue in ascending order from the bottom to the top of the figure at $\Delta = 0$ (stars) and 3 (dots).

for surface atoms ($\alpha', \alpha'' \neq \alpha$). The solution of this problem is well known to result in the surface Tamm states for electrons [11].

However, even mathematically the analogy between photons and electrons in the finite periodical potential is not complete. The important difference is that, as a reasonable approximation, the lifetime of the surface electron can usually be taken to be infinity. In other words, the decay of the surface electron excitation can be neglected. However, in the case of photon states, the decay of the surface excitations cannot be neglected even in the first order approximation and must be directly taken into account.

Let us first neglect any decay processes, by setting $\gamma_0, \gamma_0', \gamma_0'' = 0$. We also assume that the boundary conditions at both ends are identical and set $\alpha' = \alpha''$ as well as $\beta' = \beta'' = \beta$. We analyse the change of the energy levels in dimensionless units $(\omega - \omega_0)/\beta$ (ω_0 is the eigenfrequency of the single defect) versus the parameter $\Delta = |\alpha - \alpha'|/\beta$ which describes the asymmetry of the surface potential. The energy levels are shown in figure 2(a). Figure 2(b) presents the absolute value of the wavefunctions, $|\Psi_i|$, at $\Delta = 0$ (stars) and 3 (dots). Here the panels from the bottom to the top of the figure show the eigenfunctions for each eigenvalue, ω_i ($i = 1{:}5$), in ascending order. We can see that, for large enough $\Delta > 1$, two states move out of the allowed band, determined by $|(\omega - \omega_0)/\beta| < 2$ from equation (4). These states are characterized by the complex wavevector k and localized at the surface as shown in figure 2(b) (dashed lines in the two lowest panels). If the value of Δ increases further the two surface states almost completely overlap in frequency. It is clear that the number of the surface states depends on the number of defects seating on the surface. If we assume that $\alpha' \neq \alpha$ and $\alpha'' = \alpha$, that is, the eigenvalue of one surface defect remains unchanged, then only one state will move into the bandgap generating the surface mode.

Next we take into account the decay of the defect states by assuming that $\gamma_0, \gamma_0', \gamma_0'' \neq 0$. The parameter Δ is complex now, $\Delta = \Delta_r + \mathrm{i}\Delta_{\mathrm{im}}$. To show the effect of decay clearly we keep the real value of Δ equal to 2 and vary its imaginary part only. The matrix in equation (7) becomes non-Hermitian. Therefore all the eigenvalues of the structure are characterized both by the real part (the frequency ω_i), and by the imaginary part (the width of the level $\Delta\omega_i$).

The relative shifts of the energy levels versus Δ_{im} are shown in figure 2(c). In this case, the wavefunctions $|\Psi_i|$ are similar to that for $\gamma = 0$ and $\Delta = 3$ shown by dashed lines in figure 2(b). We can see that with increase in the decay of the surface photon the two surface states move towards the band edge. The width of the surface states (not shown) increases with Δ_{im} almost linearly.

We can conclude that in the one-dimensional model, similar to the Tamm surface states for electrons, the SBSs for photons are the direct consequence of the asymmetric termination of the periodic potential at the surface, $\alpha', \alpha'' \neq \alpha$. They will appear as soon as the eigenvalue difference between the surface defect and the other interior defects is larger than the coupling constant, i.e. $|\alpha' - \alpha| > \beta$. Since the coupling constant β determines the width of the allowed band directly, the Tamm states are more likely to occur for structures with narrow allowed band or with large distance between the atoms. The situation is quite different for the Shockley surface states which appear when atoms in the crystal are close to each other and interact strongly. The underlying assumption of the Shockley model is that the wavefunction of electrons should be approximated by a linear combination (hybrid orbital) of modes involving more than one wavefunction of each atom [12]. It is therefore no longer sufficient to treat each energy band as originating from a single atomic level as in the case of the Tamm states. For most semiconductors, the assumption of the hybrid orbitals is very reasonable. For example, in Si and Ge the s and p orbitals give rise to the valence and conduction bands. In the one-dimensional case of a chain composed of identical defects, the band spectrum is built on identical defect modes; therefore, no hybrid orbitals can exist. As we show below it is easy to extend our theoretical approach to a two-dimensional PC composed of identical rods. In this case, the existence of hybrid orbitals implies multi-mode resonators with coupling between different modes on the nearest neighbours as strong as the shift in frequency between the modes. Without special engineering of the unit cell this situation is very unlikely in PCs. Because of this, the link between the underlying physics of the SBSs of PCs and the Shockley surface states of electronic crystals mentioned in a number of papers [3, 4, 10] is not justified. We showed theoretically above that the properties of the SBSs in the one-dimensional case are very closely related to the Tamm surface states. We will verify the results of our theoretical analysis through the numerical 'experiment', the FDTD simulation.

3. Numerical results

We investigate how the spectrum of the five-defect chain is affected by its termination. In order to study the dependence of the defect states on the width of the allowed band, we vary the defect separation from $2a$ to $3a$ to $4a$. Figure 1 shows three structures investigated for the defects separated by $2a$.

As a model we consider a two-dimensional PC of a square lattice made of infinitely long silicon rods ($\epsilon_r = 11.9$) with radius $R = 0.35a$ embedded in vacuum ($\epsilon_0 = 1$), where a is the lattice constant. The plane-wave calculations show that this crystal prohibits propagation of the TM mode (the magnetic field is in plane and the electric field is parallel to the rods) in the frequency range $\tilde{\omega} = \omega a/2\pi c = 0.214{:}0.264$. Decreasing the radius of a single rod to $0.2a$ creates a resonant cavity. Using the super-cell plane wave technique we found that this cavity supports a non-degenerate mode at frequency $\tilde{\omega}_0 = \omega_0 a/2\pi c = 0.23$, almost exactly in the middle of the bandgap.

In order to analyse this structure, we use the FDTD technique [18]. Our computational domain is shown in figure 1. Each unit cell was divided into 20×20 discretization grid cells. The computational domain was surrounded by perfect matched layers (grey rectangular boxes), with the thickness corresponding to 10 layers of the discretization grid. The time step was

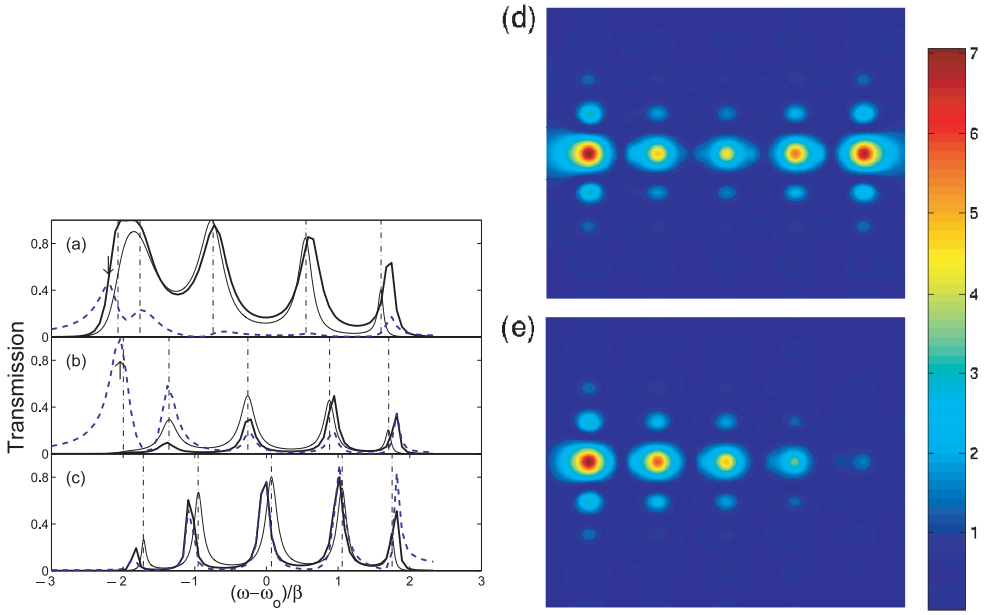

Figure 3. Transmission of the five-defect chain with the defects separated by $2a$. The response functions calculated from the FDTD simulations at ports 1 (thick solid line) and 2 (dashed line) for structures 1–3 are shown in (a), (b), and (c), respectively. The transmission coefficient of the structure found from equation (6) (thin lines) and the related spectrum calculated from equation (7) (dash–dotted vertical lines); the $|E_z|$ of structures 1 (d) and 2 (e) at the resonant frequencies indicated by arrows in (a) and (b), respectively.

$\Delta t = 1/(2\Delta xc)$. The numerical simulations were performed with the total number of time steps of 100 000. A Gaussian beam was launched at the input of the structure (S in figure 1). The spatial width of the beam was equal to 20 grid cells. A frequency spectrum of the source covered the region of interest $\Delta\tilde{\omega} = 0$–0.4. In our numerical simulations we collect a signal at ports 1 and 2.

Figure 3 presents the results of the FDTD simulations for the five-defect chain with the defect distance of $2a$. The response function calculated at ports 1 (solid line) and 2 (dashed line) for structures 1–3 is shown in figures 3(a)–(c), respectively. In order to see the relative shift of the surface states with respect to the band-edge clearly, we plot the transmission as a function of dimensionless frequency, $(\omega-\omega_0)/\beta$. In numerical analysis, the frequency ω_0 is the frequency of defect located in the centre of the calculation domain. For reference, the coupling constants of the chains with defects separated by $2a$, $3a$, and $4a$ are equal to 0.0055, 0.0021, and 0.0012, respectively. (Note that these values are in perfect agreement with the scaling law [19] of the tight-binding model, $\beta \sim 1/d^2$.) The distributions of the $|E_z|$ of structures 1 and 2 at the resonant frequencies pointed out by arrows in figures 3(a) and (b) are demonstrated in figures 3(d) and (e), respectively.

As shown above, the number of the eigenstates should be equal to the number of the defects for any chain. However, for certain boundary conditions one or two states can fall into the forbidden band, becoming the surface state. We can see that for structure 3 with no defects sitting on the crystal surface all five states are clearly visible in the spectrum of the both ports (figure 3(c)). For structures 1 and 2, we can identify four states at port 1 (solid line), while all five states are revealed at port 2 (dashed line). In structures 1 and 2 both end-defects (or one

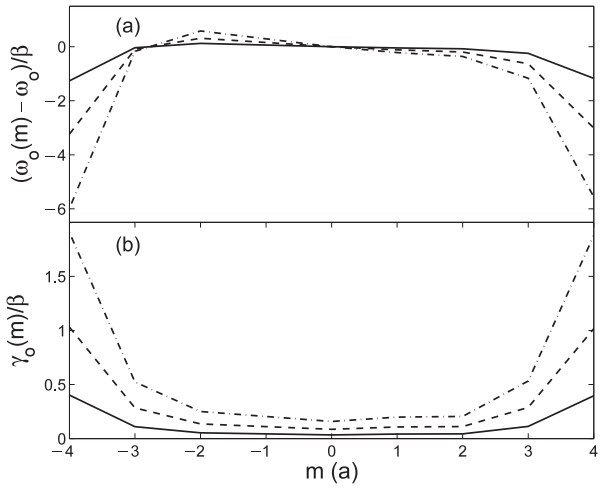

Figure 4. Dependence of the defect level shift (a) and width of the resonant peak (b) normalized to the coupling constant as a function of the defect position with respect to the centre of the crystal. Solid, dashed, and dash–dotted lines correspond to defect separations of $2a$, $3a$, and $4a$, respectively.

of them) are located on the crystal boundaries. Presumably the eigenvalues of these boundary defects should differ from those of the other defects. If the shift of the eigenvalue of the surface defect is as much as the value of β, two or one eigenstates should move away from the allowed band. We can see from figure 3(a) that structure 1 gives an example of $\Delta \geqslant 1$, where one of the surface levels has moved out of the allowed band and another state is just about to do this (see figure 2(a)). The field distributions for the lowest frequency states confirm that they are associated with the defects localized at the surface (figures 3(e), (d)).

In order to perform a theoretical modelling of this structure, we have to know how the eigenvalues of the defect (α' and α'') change when it moves along the chain. Using the FDTD simulations we determined the frequency $\omega_0(m)$, and the width, $\gamma_0(m)$, of the defect level located at different sites m of the host crystal. In order to see the eigenvalue change with respect to the width of the allowed band we normalize it to the value of β. The dependence of the defect level shift, $(\omega_0(m) - \omega_0)/\beta$, and the width of the resonant peak, $\gamma_0(m)/\beta$, as a function of the defect position with respect to the centre of the crystal are shown in figures 4(a) and (b), respectively. The data for the chains with defects separated by $2a$, $3a$, and $4a$ are represented by solid, dashed, and dash–dotted lines, respectively. We can see that the frequency of the defect is decreasing from the centre of the crystal to the surfaces. Simultaneously, the width of the resonance peak is increasing. The smaller the coupling constant β, the larger the relative shift of the level and its width.

Using the data presented in figure 4 we found the values of α' and α''. For structure 1 $\alpha'/\beta = -1.3 - \mathrm{i}0.41$ and $\alpha''/\beta = -1.2 - \mathrm{i}0.39$ while for structure 2 $\alpha'/\beta = -1.4 - \mathrm{i}0.46$ and $\alpha''/\beta = 0 - \mathrm{i}0.03$. In order to calculate the transmission coefficient from equation (6) we also have to estimate another *a priori* unknown coefficient $c_\tau\tau$ determined by the reflection on both sides of the structure. We found the factor $c_\tau\tau$ by matching the maximum of the transmission obtained from the FDTD simulation with the theoretical data obtained from equation (6). Then the theoretical transmission coefficient and related spectrum of the structure were calculated from equation (6) and equation (7), respectively. The results for the theoretical transmission coefficient of structures 1, 2, and 3 are shown by thin lines in figures 3(a), (b),

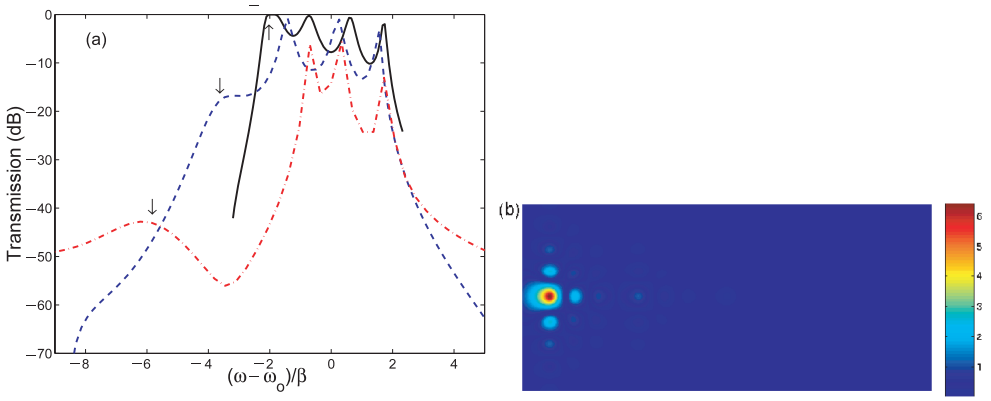

Figure 5. (a) The transmission coefficient calculated from the FDTD simulations for structure 1 with defect separation $2a$ (solid line), $3a$ (dashed line), and $4a$ (dash–dotted line). The arrows point to the surface modes. (b) The $|E_z|$ of structure 1 with defects separated by $4a$ at the resonance frequency indicated by the arrow.

and (c), respectively. The calculated band spectrum is shown by vertical dash–dotted lines. We can see that the peaks in the theoretical transmission coefficient exactly coincide with the band levels (dash–dotted lines). This validates the consistency of the developed theoretical model. Moreover, the theoretical spectrum of the defect chain exactly predicts the appearance of the surface states (see dash–dotted lines in figures 3(a) and (b)). A comparison between the theoretical calculations and the FDTD simulations shows an overall good agreement. The noticeable discrepancies between the theoretical data and the simulation results lie in error of estimating the parameters α' and α''. We would also like to mention that no fitting has been used here. We believe that these facts validate the applicability of the developed theoretical model.

As was mentioned before, the Tamm states are more likely to occur in the case of the narrow allowed band or for large distance between the atoms. Therefore we should expect that the Tamm surface state will move farther away from the band edge for the narrower band, or for the defect chains of large separation. The transmission coefficients calculated from the FDTD simulations for structure 1 with defect separation $2a$ (solid line), $3a$ (dashed line), and $4a$ (dash–dotted line) are presented in figure 5(a): the arrows point to the surface modes. The corresponding field pattern for structure 1 with defect separation $4a$ at the resonance frequency indicated by the arrow is shown in figure 5(b). We can see that, with increasing distance between the defects or with decreasing width of the allowed band (4β) the surface mode moves deeper inside the bandgap, and becomes more strongly localized to the surface (compare figures 3(d), (e) and figure 5(b)). However, the narrower the allowed band and therefore the deeper the surface mode gets inside the bandgap, the broader the width of the resonance state with respect to the allowed band is (figure 5(a)). Comparing the dash–dotted line with dashed and solid lines in figure 5(a) we can conclude that the transmission is decreasing with increasing distance between the defects in the chain. This is a direct consequence of the surface state falling deep inside the bandgap.

As mentioned in the introduction, the dependence of the surface mode on the distance between dielectric layers was first demonstrated for a multilayer structure (or a one-dimensional PC) [3]. The authors attempted to connect the SBSs with the electronic Shockley states although they were not able to explain the dependence of the surface level on the separation

between the layers using the Shockley theory. From the results of our analysis we can conclude that the SBSs of the defect chain are closely related to the Tamm surface states, rather than the Shockley states in solids.

4. Discussion

In the previous sections we demonstrated the Tamm surface states in a simple one-dimensional defect chain in a host PC. In such a structure the SBSs are localized on the ending defects, just as in the case of the original Tamm or Shockley model, with no propagation perpendicular to the chain. A question arises: are the properties of the surface states of such a defect chain studied similar to those of the propagating surface waves on a two-dimensional PC surface? Or are the results of such a model study relevant to surface Bloch waves in a real 2D or 3D PC? Again, here the analogy with the regular solid state is valid. In solids, it was realized after Tamm's and Shockley's original work for a one-dimensional model that their surfaces states localized at ends of a one-dimensional chain become surface waves in real three-dimensional solids. Many interesting properties and their applications, and indeed the whole field of surface science, emerged from their original works [13]. The relationship between localized surface states in one dimension and surface waves in two and three dimensions follows the same logic.

Our approach and the results of section 2 can be straightforwardly extended to a two-dimensional square lattice composed of identical rods. Using the transfer matrix approach [21] in terms of the empirical tight-binding model [22], we can associate each cylinder of the crystal with a Mie resonance. As we discussed in section 2, one of the conditions for the Tamm surface states is that the hybridization in the spectrum should be weak. In terms of the tight-binding model it was shown that the coupling between different Mie resonances of a PC composed of identical rods is very weak (at least for the lowest bands) [22]. Then the spectrum of the PC slab with N layers associated, for example, with the $n = 0$ (s-like) Mie resonance will be described by an equation similar to (7). But in this case, the diagonal matrix elements α must be replaced by $\alpha_0 + 2\beta_0 \cos(qa)$, where q is the momentum in the plane of the layer and a is the lattice constant of the crystal. For each q, the width of the allowed band of an infinite crystal remains equal to $4\beta_0$, with all eigenstates of the N-layer slab being shifted by $2\beta_0 \cos(qa)$ with respect to the states of the defect chain studied. In the case of the finite crystal, we have to assume that the eigenstates (or Mie resonances) of the surface cylinders differ from those of the interior cylinders. Therefore, the diagonal matrix elements of the first and last rows of matrix (7), $\alpha_0' + 2\beta_0' \cos(qa)$, must differ from those for the interior ones, or $\alpha_0 \neq \alpha_0'$, and $\beta_0 \neq \beta_0'$. Depending on the value of $\alpha_0 - \alpha_0'$, the surface states may appear either inside the bandgap or inside the allowed bands. From this analysis we can see that the essential physics of the surface states of two-dimensional PCs will be similar to that of the defect chain studied in section 2, but with one important consequence: the localized SBSs will become surface waves propagating along the surface. A more detailed study of specific realization of surface waves in higher dimensional PCs is beyond the scope of this paper.

In this paper we have discussed only the structures terminated by complete rods. Our analysis showed the existence of the surface modes even for a PC terminated by 'complete rods'. However, as was mentioned in the introduction, other studies have shown that surface states can only exist for PCs terminated by hemicylindrical rods [6] or for the surfaces with a surface rod-layer of smaller radius [9]. Remarkably, this effect can be easily explained in terms of the theory developed here. Indeed, the hemicylindrical termination or the surface monolayer should be considered rather as a defect or ad-atom layer on the surface of a crystal. We expect that such a layer gives the strongest perturbation on the surface (because a defect with half the radius of the host rods results in a state almost in the middle of the bandgap), while the

perturbation by surface rods smaller or larger than the hemicylinders should not be as strong. One of the results of the theory is that the stronger the perturbation on the surface is, the deeper the surface state moves inside the bandgap. In the case of weak perturbation or 'complete rod' termination, the surface state will almost overlap the allowed band, making surface states invisible in the experiment. Cutting the surface rods (or decreasing the radius) will increase the perturbation on the surface and move the surface state deeply inside the band gap.

As was mentioned, defect chains we studied here do not have dispersion parallel to the surface of the crystal. Therefore, depending on the component of the light momentum parallel to the surface, exactly the same mode could be either radiative or evanescent. Because of this we were able to observe the surface modes even in the transmission spectrum. We showed that, in general, the surface states on PCs are characterized by a strong decay. However, the decay could be considerably decreased by exciting the evanescent surface mode only or by using a special geometry of the surface [23].

5. Conclusion

We have studied theoretically and numerically the SBSs of a chain of identical defects embedded in a host PC. Using the FDTD simulations we analysed the genesis of the surface states. We used a comprehensive tight-binding approach to demonstrate that the surface states are a consequence of the asymmetric termination of the periodic potential at the surface. They appear as soon as the perturbation on the surface or the eigenvalue difference between the surface defect and the interior defects is larger than coupling constant, $|\alpha' - \alpha| > \beta$. Our analysis confirmed that the SBSs of the defect chain are the Tamm-like surface states. The smaller the width of the allowed band or the stronger the perturbation on the surface, the deeper the surface state moves inside the bandgap, and becomes more strongly localized to the surface. We showed that the surface states lying deep inside the bandgap affect directly the transmission through the structure. Such surface states could efficiently trap the incident light, resulting in a very low transmission. We believe that this effect should explain a well known fact of low transmission through the narrow allowed band in PCs [20].

Finally, the comprehensive theoretical model developed here proves to be capable of analysis and prediction of the properties of the SBSs on PCs giving insight into their general properties. We believe that such a detailed understanding of the governing parameters of the surface states will help to design PC surfaces with desired properties for many applications including sub-wavelength optics.

References

[1] Vlasov Y A, Moll N and McNab S J 2004 *Opt. Lett.* **18** 2175
[2] Arnaud J A and Saleh A A M 1974 *Appl. Opt.* **13** 2324
[3] Yeh P, Yariv A and Hong C-S 1977 *J. Opt. Soc. Am.* **67** 423
[4] Yeh P and Yariv A 1978 *Appl. Phys. Lett.* **32** 104
[5] Meade R D, Brommer K D, Rappe A M and Joannopoulos J D 1991 *Phys. Rev.* B **44** 10961
[6] Robertson W M, Arjavalingam G, Meade R D, Brommer K D, Rappe A M and Joannopoulos J D 1993 *Opt. Lett.* **18** 528
[7] Elson J M and Tran P 1996 *Phys. Rev.* B **54** 1711
[8] Ramos-Mendieta F and Halevi P 1999 *Phys. Rev.* B **59** 15112
[9] Moreno E, Garcia-Vidal F J and Martin-Moreno L 2004 *Phys. Rev.* B **69** 121402(R)
[10] Enoch S, Popov E and Bonod N 2005 *Phys. Rev.* B **72** 155101
[11] Tamm I E 1932 *Phys. Z. Sowiet.* **1** 733
Tamm I E 1932 *Z. Phys.* **76** 849
[12] Shockley W 1939 *Phys. Rev.* **56** 317

[13] Many A, Goldstein Y and Grover N B 1965 *Semiconductor Surfaces* (Amsterdam: North-Holland Publishing Company)
[14] Malkova N and Ning C Z 2006 *Phys. Rev.* B **73** 113113
[15] Markis K G, Suntov S, Christoulides D N, Stegeman G I and Hanche A 2005 *Opt. Lett.* **30** 2466
Smirnov E, Stepic M, Ruter C E, Kip D and Shandarov V 2006 *Opt. Lett.* **31** 2338
Molina M I, Vicencio R A and Kivshar Y S 2006 *Opt. Lett.* **31** 1693
Rosberg C R, Neshev D N, Krolikowski W, Mitchell A, Vicencio R A, Molina M I and Kivshar Y S 2006 *Phys. Rev. Lett.* **97** 083901
[16] Stefanou N and Modinos A 1998 *Phys. Rev.* B **57** 12127
[17] Reynolds A L, Peschel U, Lederer F, Robertson P J, Krauss T F and de Maagt P J I 2001 *IEEE Trans. Microw. Theory Tech.* **49** 1860
[18] Taflove A and Hagness S C 2000 *Computational Electrodynamics: The Finite Difference Time Domain Method* (Boston, MA: Artech House)
[19] Malkova N and Ning C Z 2005 *Appl. Phys. Lett.* **87** 161113
[20] Baba T and Nakamura M 2002 *IEEE J. Quantum Electron.* **38** 909
[21] Lee D H and Joannopoulos J D 1981 *Phys. Rev.* B **23** 4988–96
[22] Lidorikis E, Sigalas M M, Economou E N and Soukoulis C M 1999 *Phys. Rev. Lett.* **81** 1405
[23] Xiao S and Qiu M 2005 *Appl. Phys. Lett.* **87** 111102